

DTP/97/58  
July 1997

# Deep inelastic events containing two forward jets at HERA

J. Kwiecinski<sup>1</sup>, C.A.M. Lewis<sup>2</sup> and A.D. Martin<sup>2</sup>

<sup>1</sup> Department of Theoretical Physics, H. Niewodniczanski Institute of Nuclear Physics,  
ul. Radzikowskiego 152, 31-342 Krakow, Poland.

<sup>2</sup> Department of Physics, University of Durham, Durham, DH1 3LE, UK.

## Abstract

We use the BFKL equation to calculate the rate of deep inelastic scattering events containing two forward jets (adjacent to the proton remnants) at HERA. We compare the production of two forward jets with that of only one forward jet (the “Mueller” process). We obtain a stable prediction for this two to one jet ratio, which may serve as a measure of the BFKL vertex function.

## I. Introduction

One of the most striking discoveries at the electron-proton collider, HERA, at DESY, is the steep rise of the proton structure function  $F_2(x, Q^2)$  with decreasing Bjorken  $x \equiv Q^2/2p \cdot q$ , where  $Q^2 \equiv -q^2$ . Here  $p$  is the four-momentum of the proton and  $q$  is the four-momentum transfer of the electron probe. The behaviour of the structure function at small  $x$  is driven by the gluon through the process  $g \rightarrow q\bar{q}$ . The behaviour of the gluon distribution at small  $x$  is itself predicted from perturbative QCD via the Balitskij-Fadin-Kuraev-Lipatov (BFKL) equation, which resums the leading  $[\alpha_S \ln(1/x)]^n$  contributions. This predicts a characteristic  $x^{-\lambda}$  singular behaviour in the small  $x$  regime which results from the summation of soft multi-gluon emissions, which effectively correspond to the sum of gluon ladders (Fig. 1) where the transverse momenta  $k_{Ti}$  of the emitted gluons are unordered along the chain. For fixed  $\alpha_S$  the BFKL exponent  $\lambda = \bar{\alpha}_S 4 \ln 2$ , where  $\bar{\alpha}_S \equiv 3\alpha_S/\pi$ . It is this increase in the gluon distribution with decreasing  $x$  which produces the corresponding rise of the structure function. Of course there are uncertainties due to subleading corrections, which will reduce the value of the exponent  $\lambda$ , and from the treatment of the infrared  $k_T$  region in the numerical solution of the BFKL equation. A recent description of  $F_2$  along these lines, but also including the effects of Dokshitzer-Gribov-Lipatov-Altarelli-Parisi (DGLAP) evolution [2], can be found in ref. [3].

However, the situation is more complicated. DGLAP evolution, which resums the  $\alpha_S \ln Q^2$  contribution can on its own produce an increase in  $F_2$  with decreasing  $x$ , and with a suitable choice of input distributions at scale  $Q_0^2$  can give an excellent description of  $F_2$  at small  $x$ . This makes it difficult to distinguish whether the steep rise observed for the structure function has a major component from  $\ln(1/x)$  effects, or is simply due to  $\ln Q^2$  evolution from a non-perturbative input. The observable  $F_2$  is just too inclusive to act as a discriminator of the underlying small  $x$  dynamics.

In 1990 Mueller [5] proposed that the less inclusive quantity of DIS plus an identified energetic forward jet may serve as a useful probe of small  $x$  dynamics. The idea is to isolate DIS  $(x, Q^2)$  events containing a jet  $(x_j, k_{Tj}^2)$  with  $x \ll x_j$  and  $k_{Tj}^2 \sim Q^2$ , see Fig. 1. Here  $k_{Tj}$  and  $x_j p$  are the transverse and longitudinal momentum components of the jet. We can thus expect a  $(x/x_j)^{-\lambda}$  behaviour in a kinematic region free of DGLAP evolution<sup>1</sup>. Moreover, for large  $x_j \sim 0.1$ , the parton distributions of the proton are well known and so the Mueller proposal removes the uncertainty arising from the introduction of a non-perturbative input. That is we study DIS off a known parton, rather than off the proton. Recently data for the process have become available and the comparison with BFKL predictions is encouraging [4].

The observed DIS + forward jet data sample contains a fraction of events in which two jets are identified, each with  $p_T$  greater than the experimental cut. Our concern here is to extend the BFKL formalism to study and to estimate the rate for this process. We also present the predictions as the ratio of 1 to 2 forward jet production.

---

<sup>1</sup>The  $[\alpha_S \ln Q^2]^n$  contributions which are resummed by DGLAP come from the region in which the transverse momenta of the emitted gluons are strongly ordered along the chain, that is  $Q^2 \gg k_{Tn}^2 \gg \dots k_{Tj}^2$ . DGLAP evolution is thus neutralized by the choice  $Q^2 \sim k_{Tj}^2$ .

The structure of the paper is as follows. In Sec. II we use the data for DIS + one forward jet to determine the normalisation of our numerical solution of the BFKL equation. In Sec. III we discuss the extension of the BFKL formalism to include an extra identified gluon jet, and then in Sec. IV we present results for the cross section of DIS + two identified forward jets. Our conclusions are given in Sec. V.

## II. DIS + one forward jet

The differential cross section for deep inelastic scattering  $(x, Q^2)$  containing a forward jet  $(x_j, k_{Tj}^2)$  is of the form

$$\frac{\partial\sigma}{\partial x \partial Q^2 \partial x_j \partial k_{Tj}^2} = \frac{4\pi\alpha^2}{xQ^4} \left[ (1-y) \frac{\partial F_2}{\partial x_j \partial k_{Tj}^2} + \frac{1}{2}y^2 \frac{\partial F_T}{\partial x_j \partial k_{Tj}^2} \right] \quad (1)$$

where  $y = Q^2/sx$  with  $\sqrt{s}$  equal to the centre-of-mass energy of the electron-proton collision. The differential structure functions

$$-x_j \frac{\partial F_i}{\partial x_j \partial k_{Tj}^2} = \frac{3\alpha_S(k_{Tj}^2)}{\pi k_{Tj}^4} \left( \sum_a x_j f_a(x_j, k_{Tj}^2) \right) \Phi_i(x/x_j, k_{Tj}^2, Q^2) \quad (2)$$

where the  $\Phi_i$  represent the photon-gluon process shown by the blob in Fig. 2(a). The factor  $k_{Tj}^4$  arises from the gluon propagators. We are interested in events with small  $x/x_j$  so  $x_j$  should be taken as large as is experimentally feasible. Eq. (2) assumes strong ordering of the longitudinal momentum at the gluon-parton  $a$  vertex, so that  $x_j$  of the exchanged parton, which occurs in the parton density  $f_a(x_j, k_{Tj}^2)$ , is to a good approximation that of the outgoing jet. Assuming  $t$  channel pole dominance we have

$$\sum_a f_a = g + \frac{4}{9} (q + \bar{q}) \quad (3)$$

where  $g$ ,  $q$  and  $\bar{q}$  are the gluon, quark and antiquark densities respectively. To include the running of  $\alpha_S$  it is convenient to work in terms of the functions [6]

$$H_i(z, k_T^2) = \bar{\alpha}_S(k_T^2) \Phi_i(z, k_T^2, Q^2) \quad (4)$$

with  $i = 2, T$ . These functions satisfy the BFKL equations

$$\begin{aligned} H_i(z, k_T^2, Q^2) &= H_i^{(0)}(z, k_T^2, Q^2) \\ &+ \bar{\alpha}_S(k_T^2) \int_z^1 \frac{dz'}{z'} \int \frac{d^2 q_T}{\pi q_T^2} \left[ \frac{k_T^2}{k_T'^2} H_i(z', k_T'^2, Q^2) - H_i(z', k_T^2, Q^2) \Theta(k_T^2 - q_T^2) \right] \end{aligned} \quad (5)$$

where  $k_T'^2 = (\mathbf{k}_T + \mathbf{q}_T)^2$ . Note that the  $q_T^2 \rightarrow 0$  singularity is removed by the cancellation between the real and virtual contributions. Due to the strong ordering at the  $gaa$  vertex the

transverse momentum of the BFKL gluon is that of the forward jet, that is  $k_T^2 \simeq k_{Tj}^2$ . In eq.(5) we impose a cut-off  $k_T'^2 (k_T^2) > k_0^2$  (with  $k_0^2 \sim 1\text{GeV}^2$ ) in order to avoid the Landau pole singularity of  $\alpha_S(k_T^2)$ . The driving terms  $H_i^{(0)} = \bar{\alpha}_S(k_T^2)\Phi_i^{(0)}$  are given by the quark box (plus the crossed box) contributions to the  $\gamma g$  fusion process

$$\begin{aligned}\Phi_T^{(0)} &= \sum_q e_q^2 \frac{Q^2}{4\pi^2} \alpha_S(k_T^2) \int_0^1 d\beta \int d^2\kappa' \\ &\quad \left\{ [\beta^2 + (1-\beta)^2] \left( \frac{\kappa}{D_1} - \frac{\kappa - \mathbf{k}_T}{D_2} \right)^2 + m_q^2 \left( \frac{1}{D_1} - \frac{1}{D_2} \right)^2 \right\} \\ \Phi_L^{(0)} &= \sum_q e_q^2 \frac{Q^4}{\pi^2} \alpha_S(k_T^2) \int_0^1 d\beta \int d^2\kappa' \beta^2 (1-\beta)^2 \left( \frac{1}{D_1} - \frac{1}{D_2} \right)^2\end{aligned}\quad (6)$$

where  $\kappa' = \kappa - (1-\beta)k_T$  and

$$\begin{aligned}D_1 &= \kappa^2 + \beta(1-\beta)Q^2 + m_q^2 \\ D_2 &= (\kappa - \mathbf{k}_T)^2 + \beta(1-\beta)Q^2 + m_q^2.\end{aligned}\quad (7)$$

For small  $z$ , eq.(5) generates the characteristic  $z^{-\lambda}$  behaviour with  $\lambda = \bar{\alpha}_S 4 \ln 2$  for fixed coupling  $\alpha_S$ . DIS + forward jet events have been discussed within the BFKL formalism with fixed coupling [7].

Our objective is to calculate the ratio of DIS events containing two, as compared to one, forward jets. Since the contributions from the input  $\Phi_i^{(0)}$  largely cancel, for simplicity we do not include charm in the equations for the quark box and we assume massless quarks. In the  $z'$  integration in (5) we impose a cut  $z < z_0 \neq 1$ , such that  $x_j > x$ . This determines the point,  $z_0$ , at which the evolution in  $\ln(x_j/x)$  starts, that is the point at which the gluon chain is matched onto the quark box  $\Phi_i^{(0)}$ . Essentially, we take  $z_0$  as a free parameter which is chosen to normalise the prediction for the DIS + one forward jet cross section (as a function of  $x$ ) to the measured values. We find  $z_0 \simeq 0.5$ . If we were to enhance the driving terms by 20%, say, to allow for a charm contribution, then the starting input value  $z_0$  would be about 0.1.

To make the comparison between the prediction and the data we must impose the experimental kinematic cuts used in the measurement of the DIS + jet events. We adopt the cuts used by the H1 collaboration [4]. That is the forward jet is required to lie in the region

$$7^\circ < \theta_j < 20^\circ, \quad E_j > 28.7\text{GeV}, \quad k_{Tj} > 3.5\text{GeV} \quad (8)$$

whereas the outgoing electron is constrained to the domain

$$160^\circ < \theta_e < 173^\circ, \quad E_e > 11\text{GeV}, \quad y > 0.1 \quad (9)$$

in the HERA frame. Finally H1 require that

$$\frac{1}{2}Q^2 < k_{jT}^2 < 2Q^2 \quad (10)$$

so as to minimize the DGLAP  $\ln Q^2$  effects.

We use these cuts to calculate the DIS + forward jet cross section and compare with the H1 data in Fig. 3. We find that the choice  $z_0 = 0.5$  leads to a good description of the data. It is relevant for our study of the 2 forward jet rate to note the effect of the upper phase space cut on the variable  $y$ . The solid and dashed histograms in Fig. 3 correspond to using  $y < 0.5$  and  $y < 1$  respectively. We see that the predictions at small  $x$  are sensitive to this cut. In fact if the next smallest  $x$  bin,  $\Delta x = (0.0001, 0.0005)$  had been shown we would have seen a turnover due to the depletion of events caused by the lack of phase space.

### III. DIS + two forward jets

Here we extend the BFKL formalism so as to be able to predict the rate for the production of an extra jet in the forward direction. The process

$$\gamma^* + p \rightarrow j_1 + j_2 + X \quad (11)$$

is shown in Fig. 2(b). We require that both jets are resolved and have transverse momentum greater than some minimum cut,  $k_{Tji}^2 > \mu^2$  with  $i = 1, 2$ . The differential cross section for this process is given by

$$\begin{aligned} \frac{\partial \sigma}{\partial x \partial Q^2 \partial x_{j1} \partial k_{Tj1}^2 \partial x_{j2} \partial k_{Tj2}^2} &= \\ \frac{4\pi\alpha^2}{xQ^4} \left[ (1-y) \frac{\partial F_2}{\partial x_{j1} \partial k_{Tj1}^2 \partial x_{j2} \partial k_{Tj2}^2} + \frac{1}{2}y^2 \frac{\partial F_T}{\partial x_{j1} \partial k_{Tj1}^2 \partial x_{j2} \partial k_{Tj2}^2} \right], \end{aligned} \quad (12)$$

where the differential structure functions

$$\begin{aligned} -x_{j2} \frac{\partial F_i}{\partial x_{j1} \partial k_{Tj1}^2 \partial x_{j2} \partial k_{Tj2}^2} &= \\ \frac{1}{2\pi} \int_0^{2\pi} d\phi \Phi_i(x/x_{j2}, k_u^2, Q^2) \frac{\bar{\alpha}_S(k_{Tj2}^2) k_{Tj1}^2}{k_{Tj2}^2 k_u^2} \frac{\bar{\alpha}_S(k_{Tj1}^2)}{k_{Tj1}^4} \sum_a f_a(x_{j1}, k_{Tj1}^2), \end{aligned} \quad (13)$$

where the variables are shown in Fig. 2(b). The variable  $\phi$  is the azimuthal angle between the two forward jets. Because

$$k_u^2 = (\mathbf{k}_{Tj1} + \mathbf{k}_{Tj2})^2$$

the integral over  $\phi$  is non-trivial. The general structure of formula (13) for the production of two forward jets is readily understood as an extension of the single jet formula, (2). The

BFKL functions  $\Phi_i$  describe the gluon radiation in the upper part of the gluon emission chain, which is shown as a blob in the Fig. 2(b). These functions are obtained by solving the BFKL equation exactly as described in Sec. II, and are indeed normalised so as to describe the DIS + one forward jet data. Since both of the resolved jets are required to be in the forward region  $x_{j2} \lesssim x_{j1} \sim O(1)$ , we do not enter the strongly ordered configuration  $x_{j2} \ll x_{j1} \sim O(1)$  and so we can neglect the effect of soft (BFKL) gluon radiation emitted in the rapidity interval between the two jets. The remaining noteworthy feature of (13) is the presence of the BFKL vertex function,  $k_{Tj1}^2/k_{Tj2}^2 k_u^2$  controlling the emission of jet 2.

When the second jet is produced in the central region (that is when  $x_{j2} \ll x_{j1}$ ) then the gluon radiation in the rapidity interval between the two jets can no longer be neglected. We would need to use the formalism developed in ref. [8].

#### IV. Predictions of the DIS + two forward jet rate

We calculate the cross section for DIS + two forward jets from eqs.(12) and (13), using the kinematic cuts listed in eqs.(8-10). We present the cross section in Fig. 4. To gain insight into the effect of the cuts we also include the results obtained using the enlarged domain

$$\frac{1}{2}Q^2 < k_{Tj}^2 < 5Q^2 \quad (14)$$

for each of the two jets. For the experimental identification of two jets we require a minimum angular separation between the jets. We therefore impose a cut on the  $(\eta, \phi)$  space of the two partons producing the forward jets. For illustration we show the results for

$$\sqrt{(\Delta\eta)^2 + (\Delta\phi)^2} > R \quad (15)$$

for four different values of  $R$ , namely  $R = 0, 1, 1.7$  and  $2$ , where  $\Delta\eta$  and  $\Delta\phi$  are the differences in the pseudorapidities and azimuthal angles of the two parton jets.

From Fig. 4 we see that the two jet cross section has a turnover for the smallest  $x$  bin for the lowest set of curves, which correspond to the cut  $k_{Tj}^2/Q^2 < 2$ . The effect is not apparent when we relax the constraint to  $k_{Tj}^2/Q^2 < 5$ . Also we note that the cross section is appreciably larger for the higher kinematic cut,  $k_{Tj}^2/Q^2 < 5$ . First we quantify the increase. When we change the  $k_{Tj}^2/Q^2$  cut from 2 to 5 the cross section for DIS + single forward jet increases by a factor of about 2.5 for the smallest  $x$  bin that is shown,  $\Delta x = (0.0005, 0.001)$ , but increases only by a factor of about 1.5 for the largest  $x$  bin,  $\Delta x = (0.003, 0.0035)$ . Similarly, the cross section for DIS + two forward jets increases by factors of 5.5 and 2.5 for these two  $\Delta x$  bins respectively. The explanation for the large increase of cross section as we relax the upper limit on  $k_{Tj}^2$  from  $2Q^2$  to  $5Q^2$  can be found by inspecting Fig. 5.

Fig. 5 shows the differential cross section for DIS + two forward jets, for the  $x$  bin  $\Delta x = (0.001, 0.0015)$ , as a function of the transverse momentum of the jets, which are taken to have equal magnitude  $k_{Tj1}^2 = k_{Tj2}^2$ . We take jet resolution cut,  $k_{Tj}^2 > \mu^2$ , to be  $\mu = 3.5\text{GeV}$ . The curves on Fig. 5 correspond to the differential cross section for different values of  $Q^2$ . When

$x$ bin	$\frac{k_{Tj}^2}{Q^2} < 2$	$\frac{k_{Tj}^2}{Q^2} < 3$	$\frac{k_{Tj}^2}{Q^2} < 4$	$\frac{k_{Tj}^2}{Q^2} < 5$
0.0001 – 0.0005	1.9	7.5	15.8	25.5
0.0005 – 0.001	7.2	17.8	29.0	39.6
0.001 – 0.0015	6.0	12.8	19.4	25.2
0.0015 – 0.002	4.4	8.6	12.3	15.3
0.002 – 0.0025	3.2	5.9	8.0	9.7
0.0025 – 0.003	2.3	4.1	5.4	6.4
0.003 – 0.0035	1.7	2.8	3.7	4.3

Table 1: The dependence of the DIS + two forward jet cross section (in  $pb$ ) on the kinematic constraint  $\frac{1}{2}Q^2 < k_{Tj}^2 < nQ^2$  for various values of  $n$ . We show the dependence for different intervals of  $x$ . We take  $R = 0$ ,  $y < 1$  and  $\mu = 3.5\text{GeV}$ .

we make the cut  $k_{Tj}^2/Q^2 < 2$ , we remove a substantial contribution to the cross section from the low  $Q^2$  region. The effect is enhanced by the jet resolution cut  $k_{Tj}^2 > \mu^2$ , which requires the cross section to be zero when  $\mu^2/Q^2 < 2$ , as indicated by the vertical arrows on Fig. 5, which occur above the *lower* bound  $k_{Tj}^2/Q^2 = \frac{1}{2}$  for both  $Q^2 = 15$  and  $12\text{GeV}^2$  if we take  $\mu = 3.5\text{GeV}$ . Thus the resolution constraint has significant impact at the lower values of  $Q^2$ . The  $x$  dependence of the cross section for different kinematic constraints is shown in Table 1.

The turnover that is apparent at small  $x$  in the lower set of histograms in Fig. 4 is simply due to the lack of phase space. The reason the cross section predictions for the smaller  $x$  bins are particularly sensitive to phase space restrictions, is that such cuts kill the important low  $Q^2$  contributions, see Fig. 5.

The BFKL functions  $\Phi_i$  are common to the calculation of both the single and two forward jet rates, see eqs.(2) and (13). Thus the ambiguities in the calculation should be reduced in the prediction of the ratio  $\sigma_{2\text{jet}}/\sigma_{1\text{jet}}$ . The predictions are shown in Fig. 6, and also Fig. 7 which shows the dependence of the ratio on the jet resolution parameter  $\mu$  (but using larger  $\Delta x$  bins). As anticipated from the previous discussion we see that the ratio increases significantly when we relax the cut from  $k_{Tj}^2/Q^2 < 2$  to  $k_{Tj}^2/Q^2 < 5$ . We see that the ratio shows an increase as we move from lower to higher values of  $x$ . The reason is that the ordering  $x_{j2} < x_{j1}$  of the two emitted jets means that the reduction of the cross section due to decreasing evolution length is less for 2 forward jets than for single jet production. The ratio is insensitive to the choice of the upper limit for  $y$ . This is illustrated in Table 2 for two different jet separation cuts.

We conclude that the ratio is an observable which can give information on the underlying small  $x$  dynamics, and in particular can act as a measure of the BFKL vertex function which occurs in (13). The first experimental estimates of the ratio have been made [9], but so far only to give an indication of the size of the effect. A value of about 4% is quoted for the ratio

$\mu$ (GeV)	$R = 1.7$				$R = 2$			
	$k_{Tj}^2/Q^2 < 2$		$k_{Tj}^2/Q^2 < 5$		$k_{Tj}^2/Q^2 < 2$		$k_{Tj}^2/Q^2 < 5$	
	$y < 0.5$	$y < 1$						
3.5	3.2	3.5	7.1	7.1	2.8	3.1	6.3	6.4
5	3.2	3.6	6.7	6.9	2.9	3.2	6.1	6.2
6	3.1	3.4	6.3	6.4	2.7	3.1	5.7	5.8

Table 2: The dependence of the 2:1 forward jet ratio on the kinematical ( $k_{Tj}^2/Q^2$ ) and phase space ( $y$ ) cuts. The cross section is shown for the  $x$  bin  $\Delta x = 0.0005 - 0.002$ .  $\mu$  is the jet resolution parameter,  $k_{Tj}^2 > \mu^2$ , and  $R$  the jet separation parameter of eq.(15).

of 2-jet/1-jet events for a slightly different choice of kinematic variables than those of (8)-(10) above, namely for the domain

$$6^\circ < \theta_j < 20^\circ, \quad x_j > 0.025, \quad k_{Tj} > 5\text{GeV},$$

$$160^\circ < \theta_e < 173^\circ, \quad E_e > 12\text{GeV}, \quad 0.1 < y < 1,$$

$$0.0002 < x < 0.002, \quad \frac{1}{2} Q^2 < k_{jT}^2 < 4Q^2.$$

For this kinematic region we predict a 2-jet/1-jet ratio of 6.6% at the parton level.

A characteristic feature of the effects of the BFKL chain is the angular decorrelation of the jets [10]. Due to the lack of  $k_T$ -ordering the  $k_u$  gluon of Fig. 2(b) can bring significant transverse momentum into the two jet system and hence considerably broaden the “back-to-back” peak in the azimuthal distribution  $\Delta\phi = \phi_1 - \phi_2$ . Sample distributions are shown in Fig. 8.

In order to remove the infrared  $k_T^2 \rightarrow 0$  infinities in the BFKL equation we impose the cut  $k_T^2 = (\mathbf{k}_{Tj1} + \mathbf{k}_{Tj2})^2 > 1\text{GeV}^2$ . This, together with the ambiguity due to hadronization, means that the distribution near the back-to-back configuration cannot be predicted. Rather it is the tails of the distribution which will characterize the lack of  $k_T$  ordering. Unfortunately the jet separation cut, which experimentally is likely to be  $R \sim 1.7$ , will effectively remove the whole of the tail of the distribution, see Fig. 8. The azimuthal decorrelation is thus unlikely to be a way of identifying the underlying small  $x$  dynamics.

## V. Conclusions

The measurement of DIS scattering events  $(x, Q^2)$  containing a very forward energetic jet  $(x_j, k_{Tj}^2)$ , with  $x_j \gg x$  and  $k_{Tj}^2 \sim Q^2$ , has long been advocated as a favourable way of investigating the dynamics which underlie small  $x$  physics. The forward region is defined by cuts of the type given in eq.(8) and (9), and jet events are collected which typically lie in the region

$$\frac{1}{2}Q^2 < k_{Tj}^2 < 2Q^2 \quad (16)$$

subject also to the jet resolution cut,  $k_{Tj}^2 > \mu^2$ . To obtain sufficient statistics the first measurements take  $\mu = 3.5\text{GeV}$ , but ideally as the integrated luminosity at HERA improves, it will be preferable to obtain a DIS data sample restricted to jets with higher transverse momentum. It is already known that the DIS + forward jet data sample contains a small fraction of events with two identified jets [9]. The main purpose of this paper is to predict the fraction, and to study the properties, of these events. Our results are shown by the lower set of histograms in Fig. 6 for  $\mu = 3.5\text{GeV}$ , and in Fig. 7(a) for three different values of  $\mu$ . We see that the fraction of 2 jet events for  $R = 1.7$  is about 2.5% for the  $x$  interval  $(0.5 - 1) \times 10^{-3}$  rising to about 5% for  $x = (2.5 - 3) \times 10^{-3}$ , see Fig. 6. The fraction is rather insensitive (i) to the value of the jet resolution parameter  $\mu$ , see Fig. 7(a), and (ii) to ambiguities in the function  $\Phi_i$  describing the BFKL gluon chain since it is common to both the 1 jet and 2 jet predictions and tends to cancel in the ratio. The experimental confirmation of the predicted 2 jet fractions will therefore serve as a check on the BFKL vertex function which occurs in (13).

The domain (16) is chosen such that  $k_{Tj}^2 \sim Q^2$  so as to suppress DGLAP gluon emission. We also presented results for the larger domain  $\frac{1}{2}Q^2 < k_{Tj}^2 < 5Q^2$  simply to gain insight into the behaviour of the DIS + two forward jet cross section.

## Acknowledgements

We thank Albert De Roeck and Ewelina Mroczko for useful discussions. J.K. thanks Grey College and the Department of Physics at the University of Durham for their warm hospitality. C.A.M.L thanks the Particle Physics and Astronomy Research Council for financial support. This work has been supported in part by Polish State Committee for Scientific Research Grant No. 2 P03B 089 13, and by the EU under Contracts Nos. CHRX-CT92-0004 and CHRX-CT93-357.

## References

- [1] E.A. Kuraev, L.N. Lipatov and V. Fadin, *Zh. Eksp. Teor. Fiz.* **72**, 373 (1977) (*Sov. Phys. JETP* **45**, 199 (1977));  
Ya. Ya. Balitzkij and L.N. Lipatov, *Yad. Fiz.* **28**, 1597 (1978) (*Sov. J. Nucl. Phys.* **28**, 822 (1978));  
L.N. Lipatov, in “Perturbative QCD”, edited by A.H. Mueller, (World Scientific, Singapore, 1989), p.441;  
J.B. Bronzan and R.L. Sugar, *Phys. Rev.* **D17**, 585 (1978);  
T. Jaroszewicz, *Acta. Phys. Polon.* **B11**, 965 (1980).
- [2] Yu. Dokshitzer, *Soviet Phys. JETP* **46** (1977) 641;  
V.N. Gribov and L.N. Lipatov, *Soviet J. Nucl. Phys.* **15** (1972) 438, 675;  
G. Altarelli and G. Parisi, *Nucl. Phys.* **B126** (1977) 298.
- [3] J. Kwiecinski, A.D. Martin and A.M. Stasto, Durham preprint DTP/97/18, *Phys. Rev.* (in press).
- [4] H1 Collaboration, C. Adloff *et al.*, contributed paper pa 03-049, ICHEP '96, Warsaw, Poland, July 1996.
- [5] A.H. Mueller, *Nucl. Phys. B* (Proc. Suppl.) **18C** (1990) 125; *J. Phys.* **G17** (1991) 1443.
- [6] J. Kwiecinski, A.D. Martin and P.J. Sutton, *Phys. Rev.* **D46** (1992) 921.
- [7] W.K. Tang, *Phys. Lett.* **B278** (1992) 363;  
J. Bartels, A. De Roeck and M. Loewe, *Z. Phys.* **C54** (1992) 635;  
J. Bartels et al., *Phys. Lett.* **B384** (1996) 300.
- [8] A.H. Mueller and H. Navelet, *Nucl. Phys.* **B282** (1987) 727;  
V. Del Duca and C.R. Schmidt, *Phys. Rev.* **D49** (1994) 4510; **D51** (1995) 2150;  
W.J. Stirling, *Nucl. Phys.* **B423** (1994) 56;  
J. Kwieciński, C.A.M. Lewis and A.D. Martin, *Phys. Rev.* **D54** (1996) 6664;  
L.H. Orr and W.J. Stirling, Durham preprint DTP/97/48.
- [9] H1 collaboration: A. De Roeck, Proc. of DIS95, Paris, April 1995, eds. J.F. Laporte and Y. Sirois (Ecole Poly.) p. 309.
- [10] J.R. Forshaw and R.G. Roberts, *Phys. Lett.* **B335** (1994) 494;  
A.J. Askew, D. Graudenz, J. Kwiecinski and A.D. Martin, *Phys. Lett.* **B338** (1994) 92.

## Figure Captions

Fig. 1 Diagrammatic representation of a deep inelastic event containing an identified forward jet with longitudinal and transverse momentum components  $x_j p$  and  $k_{Tj}$  respectively. The photon scatters from the gluon chain (via the quark ‘box’) described by the BFKL equation which resums the (soft) gluon emissions. Parton  $a$  can be either a gluon or a quark.

Fig. 2 The diagrams giving the cross section for (a) DIS + one forward jet and (b) DIS + two forward jets. In each case the upper blob represents the BFKL functions  $\Phi_i$  (which in the absence of the BFKL gluon emissions would, to lowest order, be simply given by the quark box and crossed box,  $\Phi_i^{(0)}$ ). The dot represents the BFKL vertex function “measured” by the 2 jet/1 jet ratio.

Fig. 3 The DIS + forward jet cross section compared with recent H1 data [4]. The phase space cuts are given in eqs.(8-10). The resummed BFKL kernel is normalized by the choice  $z_0 = 0.5$ . The solid (dashed) histograms correspond to  $y < 0.5$  and  $y < 1$  respectively.

Fig. 4 The DIS + two forward jet cross section  $\sigma_2$  in the same  $x$  bins as for the DIS + forward jet results. We take  $y < 0.5$ .  $\sigma_2$  is plotted for  $k_{Tj} > 3.5\text{GeV}$  for two different choices of the upper  $k_{Tj}$  cut:  $k_{Tj}^2/Q^2 < 2$  and 5. The results are shown for four different cuts on the minimum separation between the two forward jets:  $R = 0, 1, 1.7$  and 2. The smaller the separation cut, the higher the cross section.

Fig. 5 The differential cross section for DIS + two forward jets as a function of  $k_{Tj}^2/Q^2$ , for different values of  $Q^2$ . We take  $k_{Tj1}^2 = k_{Tj2}^2$ ,  $k_{Tj}^2/Q^2 > \frac{1}{2}$ ,  $R = 0$  and the jet resolution cut off  $\mu = 3.5\text{GeV}$ . The cross section (12) is integrated over  $x_{j1}$  and  $x_{j2}$  and is shown for the  $x$  bin  $\Delta x = (0.001, 0.0015)$ . The lower cut-offs are indicated by vertical arrows for the different values of  $Q^2$ .

Fig. 6 The same as Fig. 4, but showing the ratio of the two/one forward jet cross section.

Fig. 7 The two/one forward jet ratio predicted for DIS events shown for three different values of the jet resolution parameter  $\mu$  (that is  $k_{Tj}^2 > \mu^2$ ), and for two upper limits of  $k_{Tj}^2/Q^2$ . The two jets are taken to have the same  $k_{Tj}^2$ . The five different histograms correspond, in descending order, to  $R = 0, 1, 1.5, 1.7$  and 2, where the jet separation parameter  $R$  is defined in (15).

Fig. 8 The cross section as a function of the azimuthal separation,  $\Delta\phi = \phi_1 - \phi_2$ , of the two forward jets. The distribution is shown for two choices of  $k_{Tj}^2/Q^2$  and for two different  $x$  bins. We take  $y < 0.5$ , and we show the distributions for  $R = 0, 1$  and 1.7, where the jet separation parameter  $R$  is defined in (15).

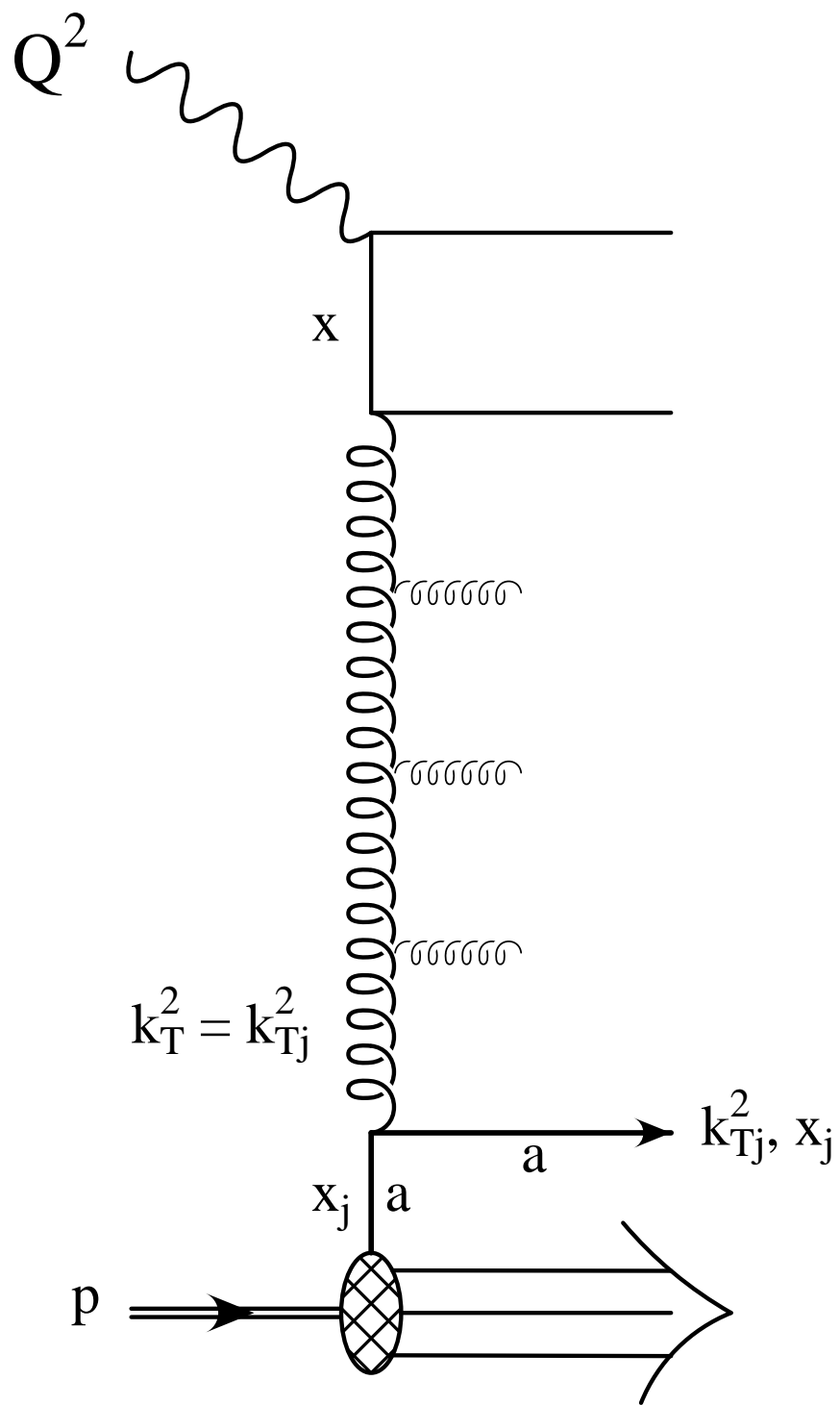
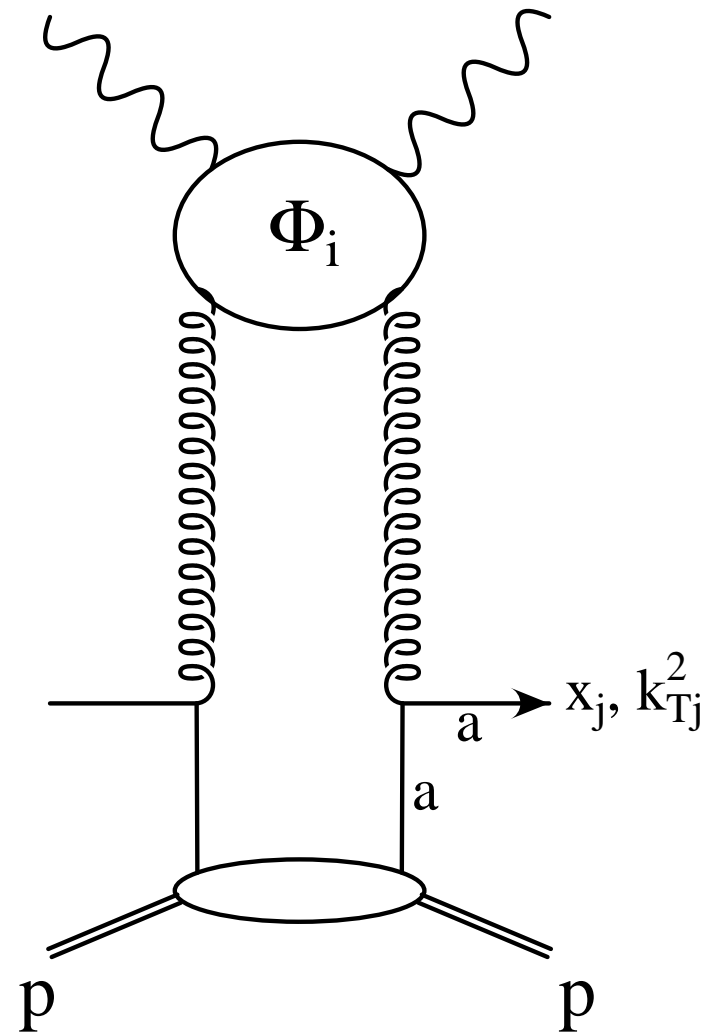


Fig. 1

(a) DIS + jet



(b) DIS + two jets

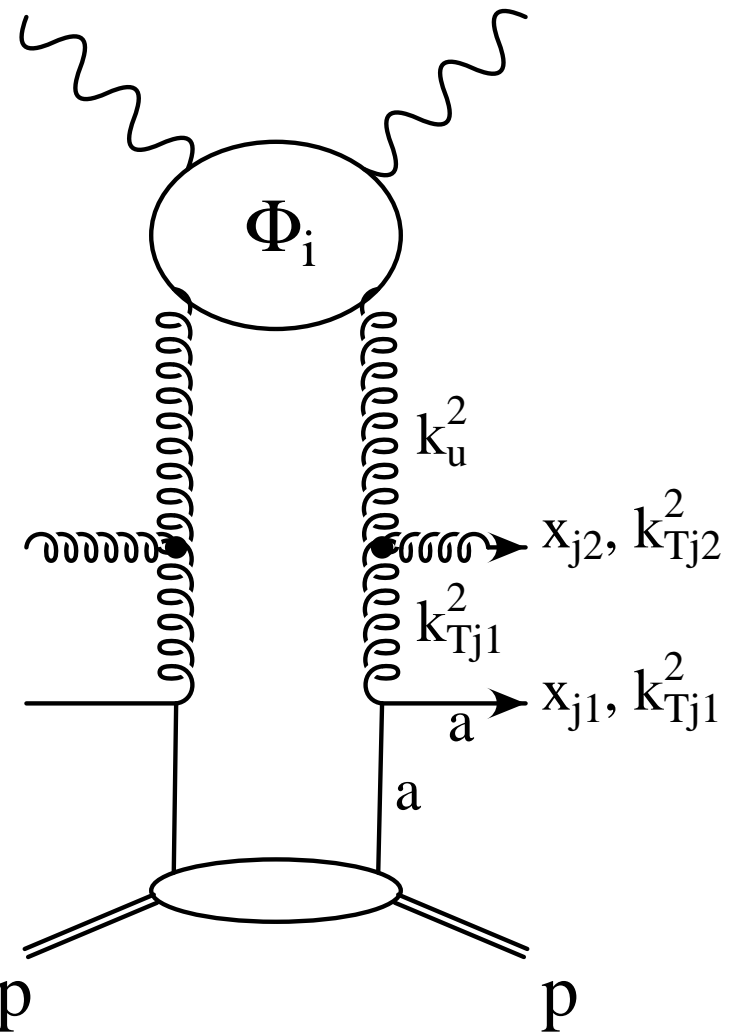


Fig. 2

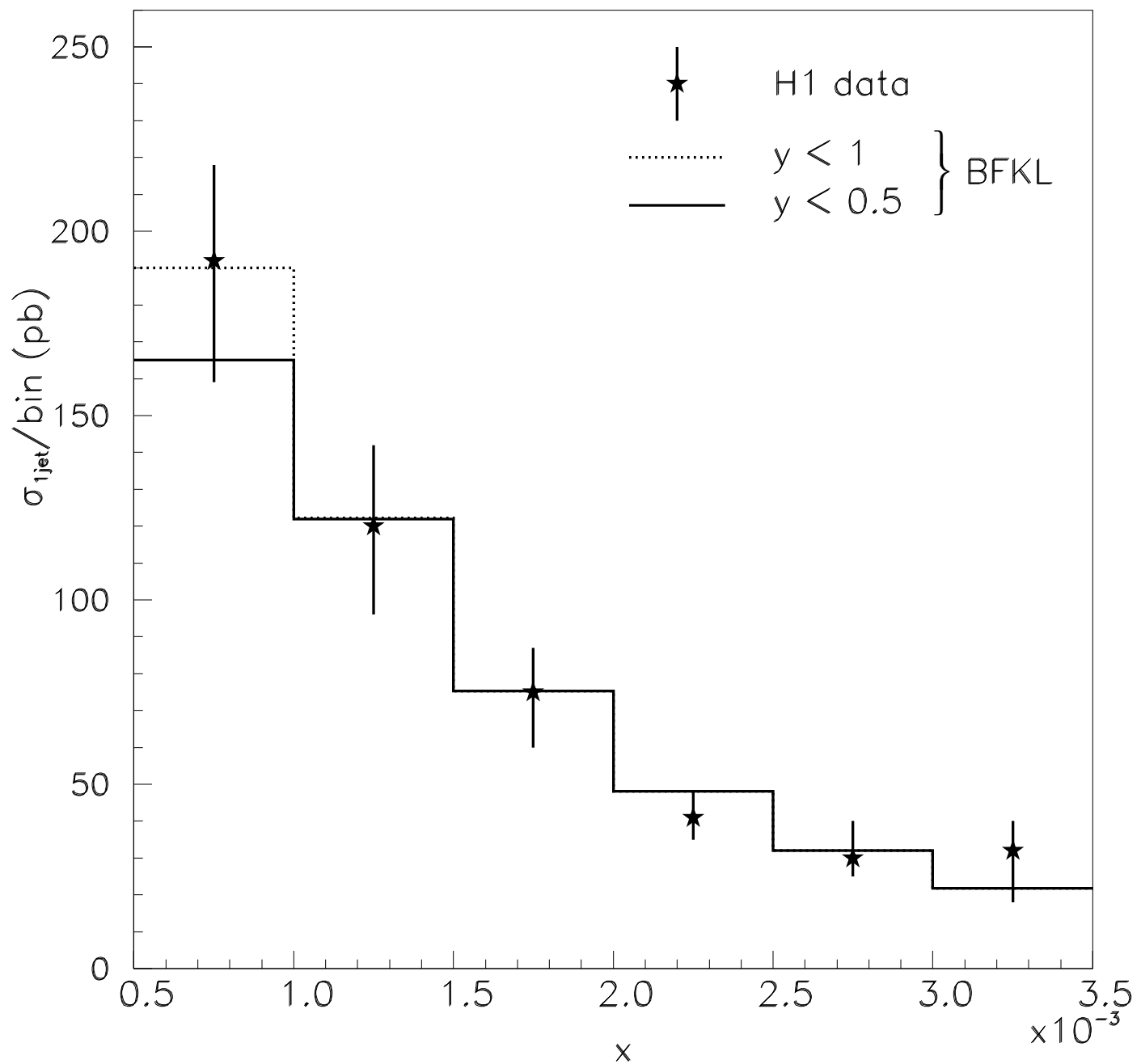


Fig. 3

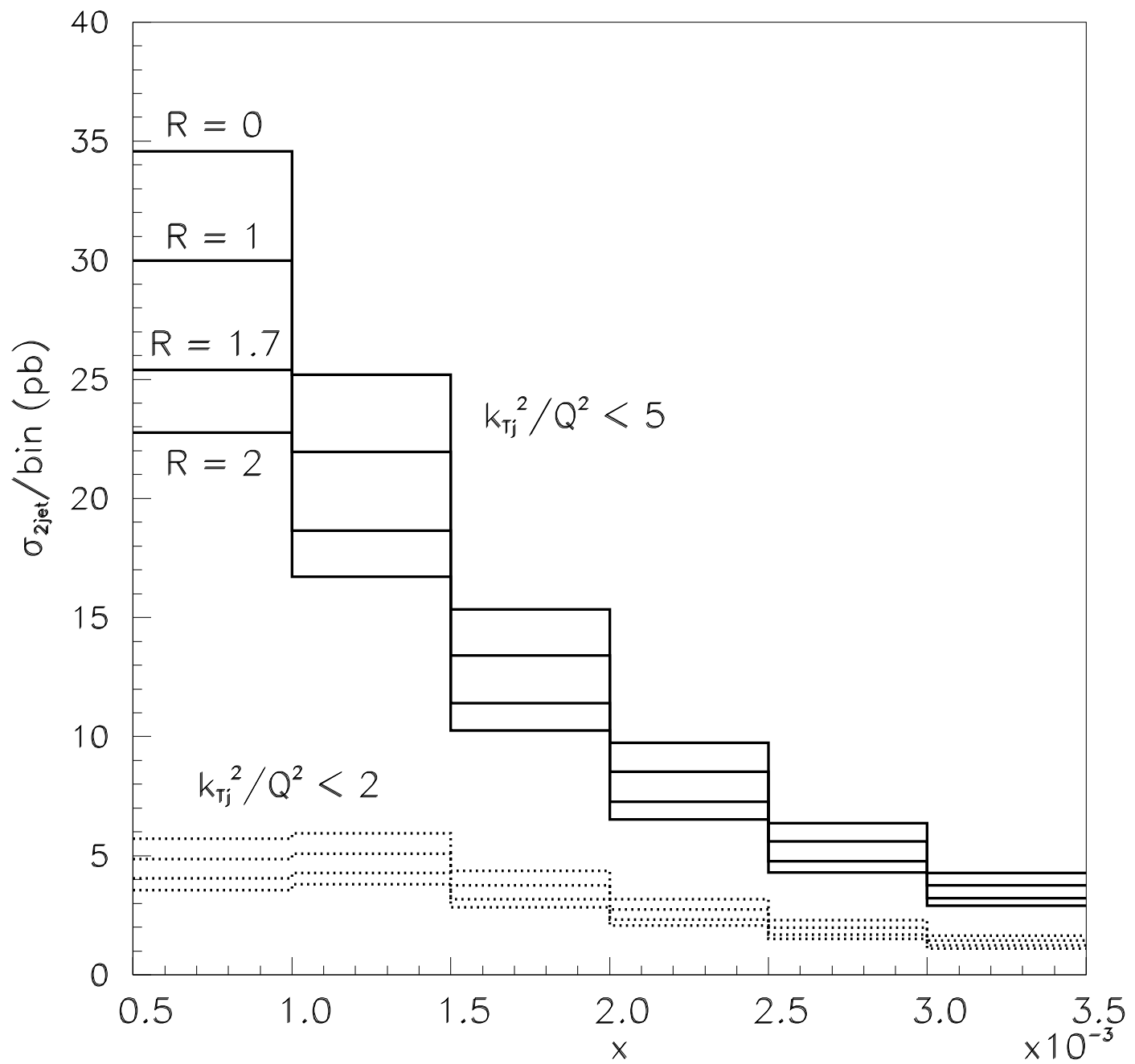


Fig. 4

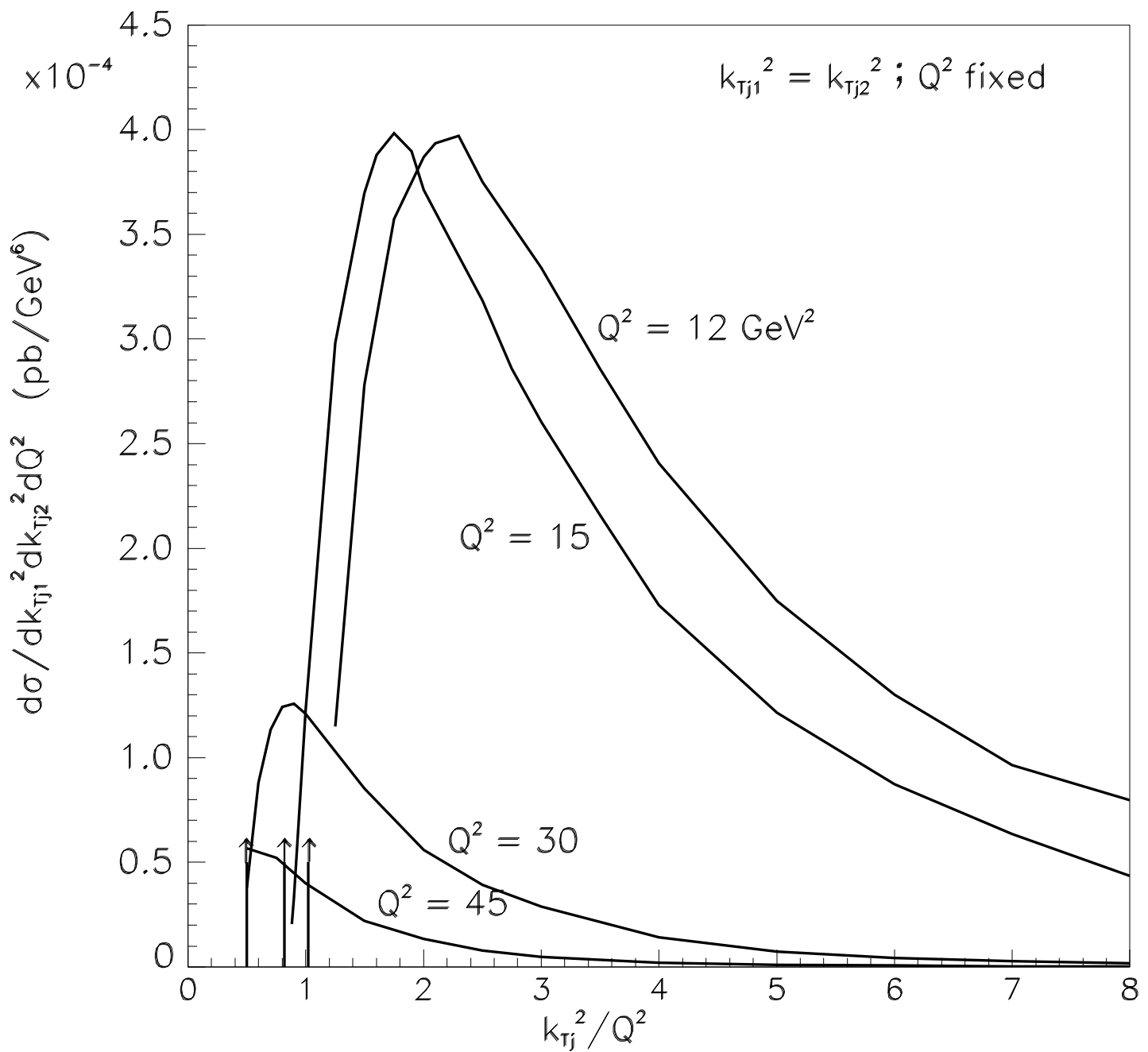


Fig. 5

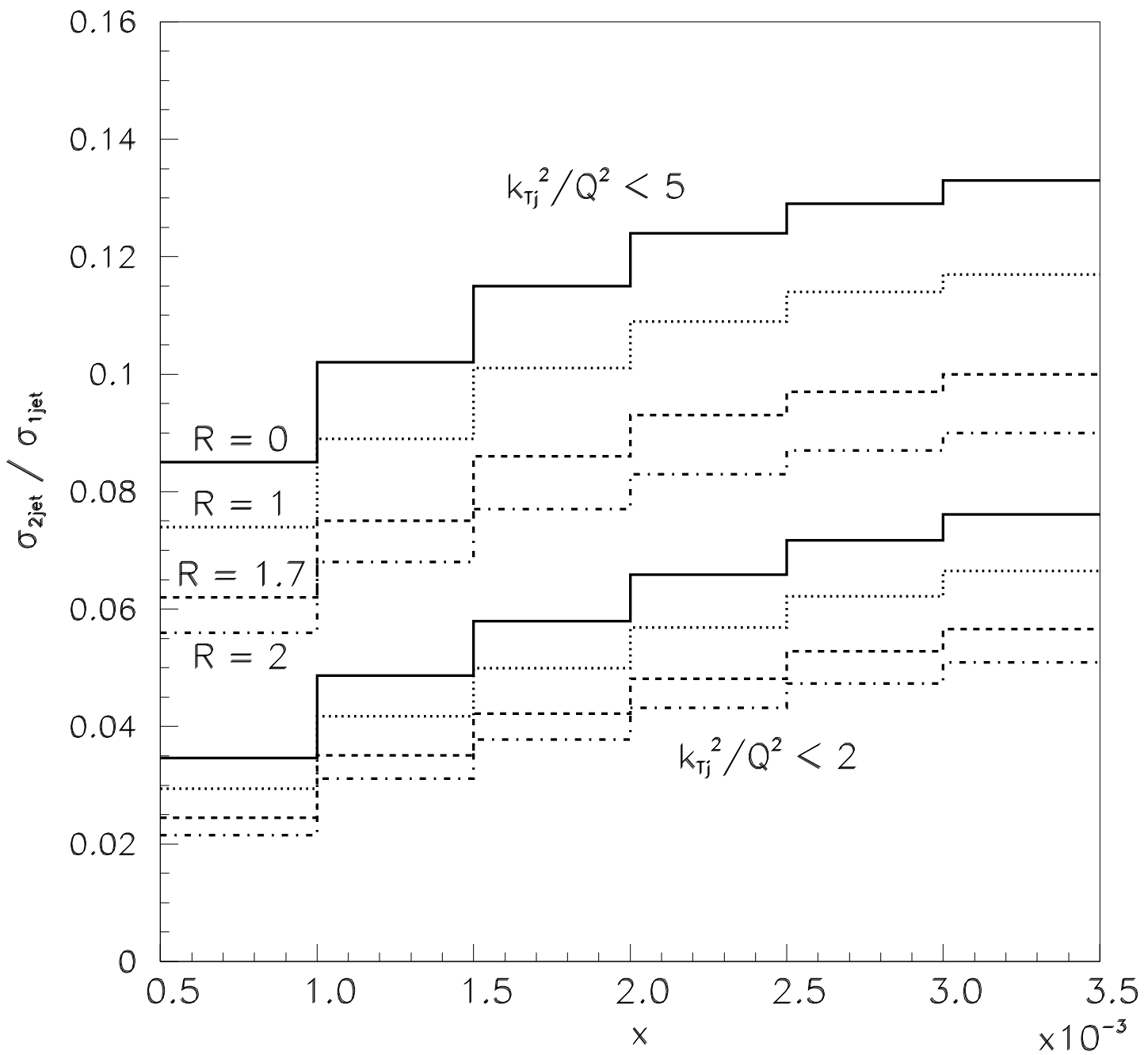


Fig. 6

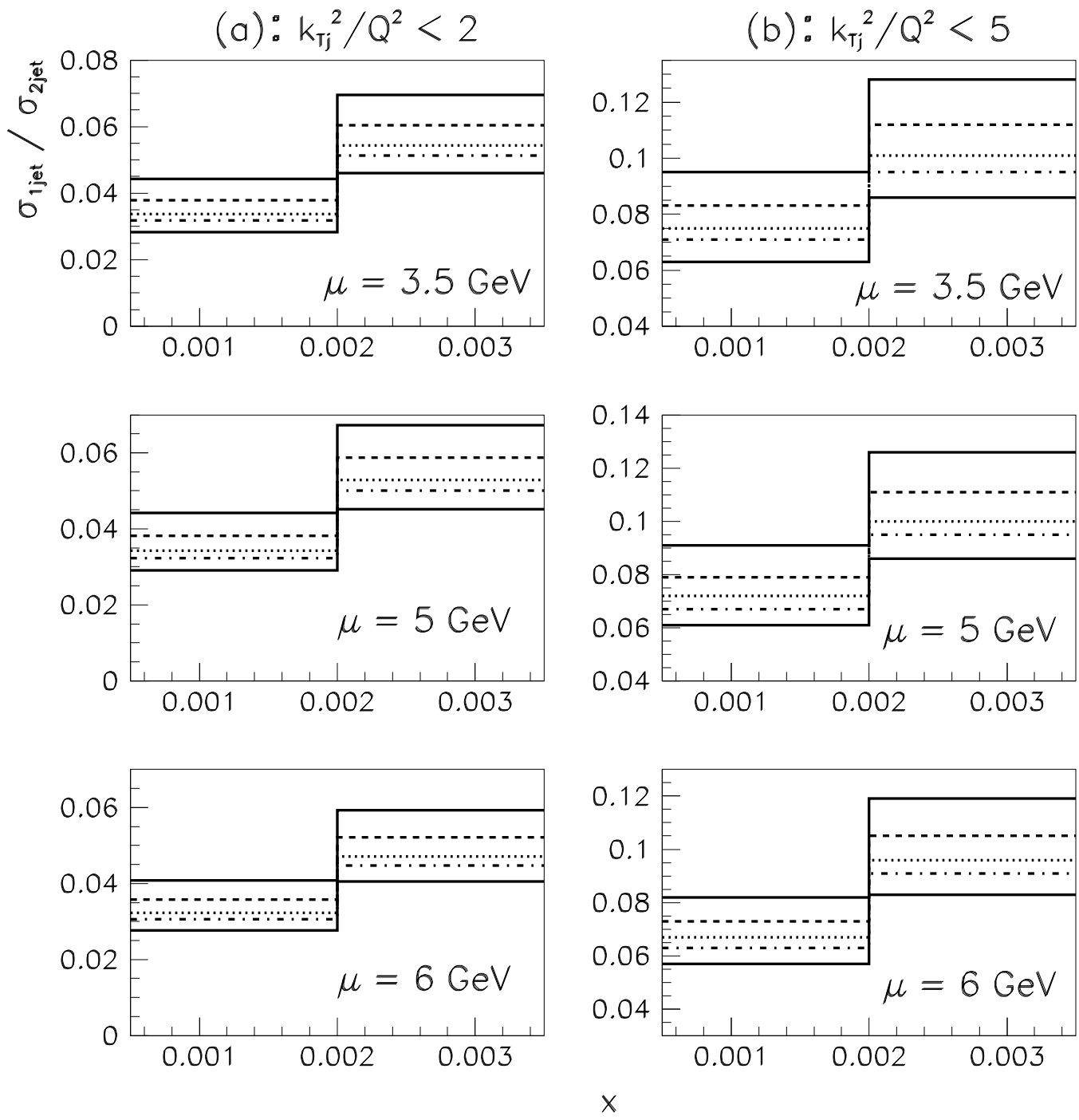


Fig. 7

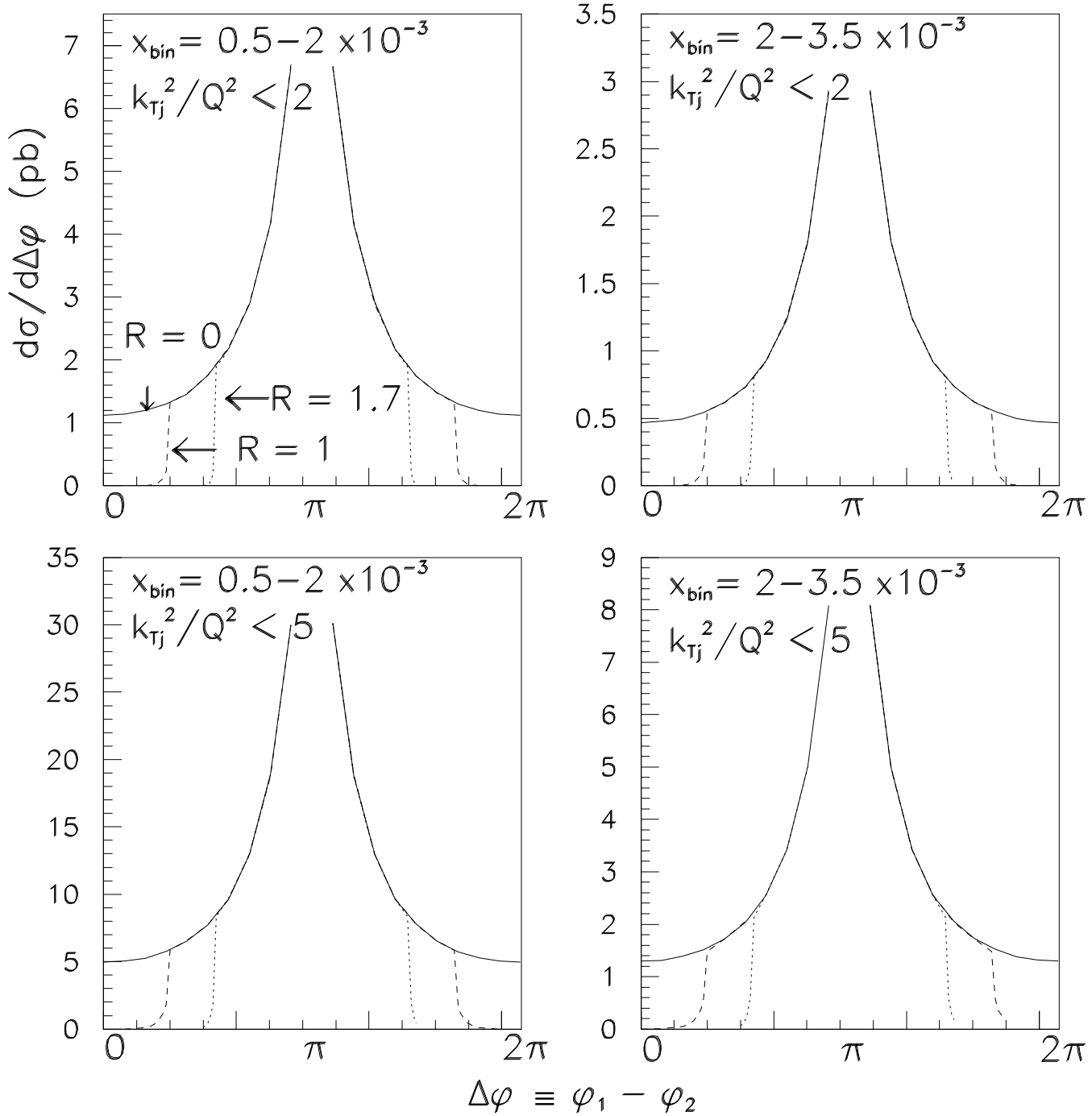


Fig. 8